NASA Technical Memorandum 106184
ICOMP–93–17

On Nonlinear Tollmien-Schlichting/Vortex Interaction in Three-Dimensional Boundary Layers

Dominic A.R. Davis
Institute for Computational Mechanics in Propulsion
Lewis Research Center
Cleveland, Ohio

and

Frank T. Smith
University College London
London, United Kingdom

May 1993

NASA

ON NONLINEAR TOLLMIEN-SCHLICHTING/VORTEX INTERACTION IN THREE-DIMENSIONAL BOUNDARY LAYERS*

Dominic A.R. Davis
Institute for Computational Mechanics in Propulsion
Lewis Research Center
Cleveland, Ohio 44135

and

Frank T. Smith
University College London
London, WC1E 6BT, United Kingdom

ABSTRACT

The instability of an incompressible three-dimensional boundary layer (that is, one with cross-flow) is considered theoretically and computationally in the context of vortex/wave interactions. Specifically the work centres on two low-amplitude,lower-branch Tollmien-Schlichting waves which mutually interact to induce a weak longitudinal vortex flow; the vortex motion,in turn,gives rise to significant wave-modulation via wall-shear forcing. The characteristic Reynolds number is taken as a large parameter and,as a consequence, the waves' and the vortex motion are governed primarily by triple-deck theory. The nonlinear interaction is captured by a viscous partial-differential system for the vortex coupled with a pair of amplitude equations for each wave pressure. Three distinct possibilities were found to emerge for the nonlinear behaviour of the flow solution downstream - an algebraic finite-distance singularity,far-downstream saturation or far-downstream wave-decay (leaving pure vortex flow) - depending on the input conditions,the wave angles and the size of the cross-flow.

1. INTRODUCTION

Our primary concern in this paper on transition is to extend the recently developed ideas on nonlinear disturbances in otherwise two-dimensional boundary layers to the more general and practical case of three-dimensional boundary layers, i.e. with cross-flow. Although some linear theory has been written where cross- flow effects have been incorporated (such as Stuart 1963, Hall 1986 on predominantly inviscid modes and Stewart and Smith 1987 on viscous-inviscid modes) little research has been performed in a nonlinear context as far as we are aware. Yet the influences of cross-flow are of particular importance in numerous aerodynamical configurations,for example on swept wings or near wing-body junctions.

Concerning flows without significant cross-flow,initially at least,in recent years evidence has accumulated that persistent streamwise vortices can play a key role as an early

*Work funded under NASA Cooperative Agreement NCC3-233.

stage in transition to turbulence of boundary layers and duct flows. In the boundary-layer context,the evidence is mainly from experimental observations (Aihara et al. 1965,1969, 1981,1985, Tani and Sakagami 1962, Klebanoff,Tidstom and Sargent 1962, Bippes and Gortler 1972),but also from supporting computational work (Wray and Hussaini 1984, Spalart and Yang 1987).

The observations have provided the stimulus for recent theoretical studies in this field notably for boundary layers (Hall and Smith 1989,1991, Smith and Walton 1989) and channel flows (Hall and Smith 1988, Bennett,Hall and Smith 1991, Smith and Blennerhassett 1992). The studies are based on the ideas of vortex/ wave interactions: this is the situation where two or more wave-like disturbances mutually interact under inertial forces in such a way as to induce a longitudinal vortex flow component. This component generally has slower streamwise and temporal variations, given that each wave has common frequency and streamwise wavenumber. If the vortex also has a significant back-influence on the waves,i.e. contributes to their growth or decay,then we have full interaction and the waves' and vortex solutions must be solved together. The interaction may be weak or strong depending on whether the oncoming mean flow is altered by a small amount or a significant amount respectively. Quite recently,the weakly nonlinear interactions arising between a pair of three-dimensional(3D) Tollmien-Schlichting (TS) waves and their induced streamwise vortices have been studied theoretically for a two-dimensional boundary layer over a flat surface by Hall and Smith (1989). The present work extends the above ideas to 3D boundary-layer profiles. Hence our main concern is with the effects of cross-flow and the role it plays,if any,in determining the ultimate nonlinear behaviour of the flow solution downstream from the input station. This is felt to be a significant problem to study mainly because,as mentioned previously,3D flows are more commonly encountered in practice.

It should be emphasized that nonlinear interactions between vortices and viscous-inviscid waves are addressed here with cross-flow present,starting from the interaction with zero cross-flow considered in Hall and Smith (1989),Smith and Blennerhassett (1992) and then gradually increasing the cross-flow. Interactions involving vortices and predominantly inviscid,Rayleigh,waves have still to be extended fully in this way,leading on eventually to the study of nonlinear interactions between mean-flow vortices and inviscid cross-flow modes. Starts on the latter extension have been made however by Davis (1992) and Brown and Smith (1992), based again on the flow structure holding for zero cross-flow as described by Davis (1992),Brown,Brown and Smith (1992),Smith,Brown and Brown (1992). One of the main findings,both in the last two works for vortex interactions with inviscid waves and in Smith and Blennerhassett (1992) for viscous-inviscid waves,is the existence of persistent vortices that emerge downstream of regions of full vortex-wave interaction in certain parameter ranges,i.e. pure vortex flow with decayed waves dominates downstream. Again,the above is mostly for vortex-wave interactions in the incompressible regime,as in the present work. The compressible boundary layer with vortex-wave interaction is treated by Bowles,Elliott and Smith (1992),concerning the effects of surface distortions,and again

they find persistent vortices to be formed quite commonly as a downstream product of nonlinear interaction. When that happens, the vortex-wave interaction (upstream) has served to alter the mean flow (downstream) to a stable one containing longitudinal vortices.

An intriguing issue is whether flow properties such as persistent downstream vortices continue when cross-flow is added,and,if so,how the parameter ranges are affected. Our particular concern is with the effects of cross-flow on vortex/TS interactions. There are several kinds of interaction in fact,even within the context of vortices with viscous-inviscid (TS) modes. One related kind is discussed by Stewart and Smith (1992),Bowles and Smith (1992),regarding flow responses at relatively high frequencies. These are sigificant because,among other things,they provide the first theoretical explanation for the Klebanoff and Tidstrom (1959) classic path of transition. Indeed,quantitative comparisons between the theory and experiments of Klebanoff and Tidstrom (see also Klebanoff,Tidstrom and Sargent 1962) in boundary layers and Nishioka et al (1979) in channel flows yield very encouraging agreement,as Stewart and Smith and Smith and Bowles show. The last reference also makes comparisons with the strongly nonlinear break-up theory of Smith (1988),for a later stage of transition,and again the theoretical-experimental agreement is good in quantitative terms.

As in Hall and Smith(1989),then,we address nonlinear disturbances sufficiently close to the first,lower-branch,neutral station. There the TS waves are governed mainly by the triple-deck structure,given that the typical Reynolds number,which is defined below,is large (Smith 1979). The structure stays intact even with cross-flow present (Stewart and Smith 1987). Moreover,if the coordinate scales controlling the vortex are taken first to be comparable with those for the wave,the above structure additionally incorporates the induced-vortex motion,as we shall see. The nonlinear evolution process is principally contained within the lower deck of the triple-deck structure wherein the velocities $u_\infty(u,v,w)$,the Cartesian coordinates $l_\infty(x,y,z)$,the pressure $\rho_\infty l_\infty^2 p$ and the time $l_\infty u_\infty^{-1} t$ are scaled in the form

$$\begin{aligned}[u,v,w,p,x-x_0,y,z-z_0,t] = [&Re^{-1/8}\tilde{u}, Re^{-3/8}\tilde{v}, Re^{-1/8}\tilde{w}, Re^{-1/4}\tilde{p},\\ &Re^{-3/8}X, Re^{-5/8}Y, Re^{-3/8}Z, Re^{-1/4}T]\end{aligned} \qquad (1.1a-h)$$

near a typical $O(1)$ station $x = x_0$,$z = z_0$ .Here $l_\infty, u_\infty, \rho_\infty, \nu_\infty$ represent,in turn,the typical streamwise length such as the airfoil chord, the flow speed in the outer stream(in the $x-$direction),the fluid density and the kinematic fluid viscosity. The global Reynolds number $Re \equiv u_\infty l_\infty \nu_\infty^{-1}$ is taken to be a large parameter. The oblique TS waves are represented by

$$E_{1,2} \equiv exp[i(\alpha X + \beta_{1,2} Z/2 - \Omega T)], \qquad (1.2a,b)$$

where α, β_1, β_2 and Ω are real constants. We note that the spanwise wavenumbers β_1, β_2 depend essentially on the crossflow evaluated at the edge of the boundary layer. This is due to the dispersion relation which stems from the dominant wave motion,as analysed in

Section 3. The waves interact nonlinearly to induce streamwise-vortex flow,in the manner $E_1 E_2^{-1} = E_3$,where

$$E_3 \equiv exp[i(\beta_1 - \beta_2)Z/2]. \tag{1.2c}$$

represents the vortex component. Equally we note the properties $E_1 E_3^{-1} = E_2$, $E_2 E_3 = E_1$ which correspond to the vortex combining with the first wave to provoke the second wave and combining with the second wave to provoke the first wave respectively.

The governing equations are the unsteady,interactive 3D boundary-layer (triple- deck) equations,written down in Section 2,and as shown in the analysis that follows that section,these equations cover both the waves' and the vortex motion,in (1.2a-c), in effect, despite the slower scales associated with the vortex. The scales and the flow structure for the TS/vortex interaction in a full 3D boundary layer are examined in Sections 3.1 to 3.5 below,for which a partial- differential system for the vortex flow coupled with an ordinary differential equation for each wave pressure is derived. These interaction equations are written down in Section 3.6 and special attention is paid to the case of zero starting vortex flow,i.e. where the input consists of only the two waves (1.2a,b) superimposed on the 3D boundary layer,since then it is possible to deduce an integral form for the downstream evolution of the vortex-streamwise wall shear. The interaction equations are addressed numerically and analytically in Section 4,and comparisons are noted therein. Three main types of nonlinear behaviour are found to occur: an algebraic finite-distance break up; far-downstream saturation of the waves' and the vortex motion; and far-downstream decay of the waves' and the vortex motion. Significantly in the last option it is found that the waves die out rapidly in an exponential manner but the vortex decays in a slow algebraic fashion and so in a sense we are left with pure vortex motion. The above options depend on the input conditions,the wave angles and the magnitude of the cross-flow. It is interesting that the numerical results reflect that the first option occurs in the majority of cases. Finally,in Section 5,the results obtained in the previous sections are discussed.

2. THE GOVERNING EQUATIONS

Substituting the expansions (1.1a-h) into the Navier-Stokes equations shows that the scaled variables are governed by the unsteady,interactive 3D boundary-layer equations

$$\tilde{u}_T + \tilde{u}\tilde{u}_X + \tilde{v}\tilde{u}_Y + \tilde{w}\tilde{u}_Z = -\tilde{p}_X + \tilde{u}_{YY}, \tag{2.1a}$$

$$\tilde{w}_T + \tilde{u}\tilde{w}_X + \tilde{v}\tilde{w}_Y + \tilde{w}\tilde{w}_Z = -\tilde{p}_Z + \tilde{w}_{YY}, \tag{2.1b}$$

$$\tilde{u}_X + \tilde{v}_Y + \tilde{w}_Z = 0, \tag{2.1c}$$

with the boundary conditions

$$\tilde{u} = \tilde{v} = \tilde{w} = 0 \qquad \text{at } Y = 0, \tag{2.1d}$$

$$\tilde{u} \sim Y + A, \quad \tilde{w} \sim Y^{-1} \qquad \text{as } Y \to \infty. \tag{2.1e}$$

Here the pressure $\tilde{p}$ and the displacement decrement A are unknown functions of X, Z and T ,linked via the expression

$$\tilde{p}(X,Z,T) = \frac{-1}{2\pi} \bar{\int}_{-\infty}^{\infty} \bar{\int}_{-\infty}^{\infty} \frac{(u_e \partial/\partial\xi + w_e \partial/\partial\eta)^2 A(\xi,\eta,T)}{[(X-\xi)^2 + (Z-\eta)^2]^{1/2}} d\xi d\eta, \qquad (2.1f)$$

arising from the main- and upper-deck analyses,where $(u_e, 0, w_e)$ denotes the basic flow outside the boundary layer. Bars on the integral signs denote the principal value or the finite part. We observe that the cross-flow influence on the above system comes exclusively from its value at the "upper edge" of the boundary layer and is felt through the pressure-displacement law (2.1f). No other cross-flow effect is felt within the lower deck because the Cartesian coordinates have been chosen in such a way that the direction of maximum basic-flow wall shear is in the "$x-$direction",implying that the basic flow has no spanwise wall shear.

3. THE ANALYSIS

3.1 The main scales

It is well known that lower-branch TS waves (linear or nonlinear) in a 3D boundary layer are governed by the triple-deck equations (2.1a-f) cited above (Smith 1979). Here,the waves have characteristically small amplitudes in comparison to their fully nonlinear size; in particular,if the relative magnitude is $\hat{h}$,where $\hat{h} \gg Re^{-m}$ (for any $m > 0$),then a vortex flow of $O(\hat{h}^2)$ is induced through nonlinear wave-coupling. It is found that the vortex-spanwise velocity grows logarithmically far from the plate's surface due to the algebraic decay (of $O(Y^{-2})$) of the wave-inertial forcing effects there. The singularity is eventually damped out in a buffer deck,lying between the main and lower decks, where the shear-inertial effects (essentially proportional to $Y|\partial_{\bar{X}_v}|$,where $\bar{X}_v$ is the modulated streamwise length scale over which the vortex and wave-amplitude variations take place) come into play. If the relative thickness of the buffer deck is $\delta(\gg 1)$ then convective-diffusive balances yield $|\partial_{\bar{X}_v}| \sim \delta^{-3}$. There $\tilde{u}_v \sim \hat{h}^2\delta^3 \ln\delta, \tilde{w}_v \sim \hat{h}^2 \ln\delta$,where $\tilde{u}_v, \tilde{w}_v$ denote the vortex-streamwise and -spanwise velocities,and continuity has been used. In Hall and Smith (1989) it was assumed (and subsequently confirmed) that sensitive nonlinear interactions would happen if the amplitude variations of the wave over the longer scale were controlled to some extent by the vortex shear from the buffer deck. Proceeding in a similar vein yields the second $\delta - \bar{X}_v$ balance $|\partial_{\bar{X}_v}| \sim \hat{h}^2\delta^2 \ln\delta$, whereupon combining with the first such balance gives

$$\delta \sim h^{-2/5}, \bar{X}_v \sim h^{-6/5}$$

where

$$\bar{h} \equiv h\left\{\frac{-2}{5}\ln h\right\}^{-1/2}.$$

Unlike the related work in Hall and Smith (1989) for zero crossflow,we have not included nonparallelism here,although it is relatively easy to incorporate these additional effects as described in Appendix A.

3.2 The lower deck

In the lower deck,where $y = Re^{-5/8}Y$,viscous forces play a prominent role: this is readily observed from the unsteady,interactive 3D boundary-layer equations which hold here,namely

$$\tilde{u}_T + \tilde{u}\tilde{u}_X + \tilde{v}\tilde{u}_Y + \tilde{w}\tilde{u}_Z = -\tilde{p}_X + \tilde{u}_{YY}, \tag{3.1a}$$

$$\tilde{w}_T + \tilde{u}\tilde{w}_X + \tilde{v}\tilde{w}_Y + \tilde{w}\tilde{w}_Z = -\tilde{p}_Z + \tilde{w}_{YY}, \tag{3.1b}$$

$$\tilde{u}_X + \tilde{v}_Y + \tilde{w}_Z = 0, \tag{3.1c}$$

$$\text{with } \tilde{p} \text{ independent of } Y, \tag{3.1d}$$

$$\text{and the no-slip condition : } \tilde{u} = \tilde{v} = \tilde{w} = 0 \text{ at } Y = 0. \tag{3.1e}$$

We refrain from applying the outer constraint (2.1e) here because,in effect,the original lower deck has split into two separate decks,characterised by the current regime and the thicker buffer deck; it is in the latter region where application of (2.1e) takes place. Here we express the flow solution in the form

$$\tilde{u} = \lambda Y + hL\tilde{u}^{(1)} + h^{6/5}\lambda_3(Z)Y + h^2L^2\tilde{u}^{(3)} + h^{11/5}L\tilde{u}_a^{(1)} + \cdots, \tag{3.2a}$$

$$\tilde{v} = hL\tilde{v}^{(1)} + h^2L^2\tilde{v}^{(3)} + h^{11/5}L\tilde{v}_a^{(1)} + \cdots, \tag{3.2b}$$

$$\tilde{w} = hL\tilde{w}^{(1)} + h^2L^2\tilde{w}^{(3)} + h^{11/5}L\tilde{w}_a^{(1)} + \cdots, \tag{3.2c}$$

$$\tilde{p} = hL\tilde{p}^{(1)} + h^{11/5}L\tilde{p}_a^{(1)} + \cdots + h^{16/5}\tilde{p}^{(3)} + \cdots, \tag{3.2d}$$

where $L \equiv \left\{\frac{-2}{5}\ln h\right\}^{-1/2}$ and λY is the basic-flow shear arising from the main deck. The terms superscripted (1) are TS contributions,with the quantities subscripted by 'a' denoting the second order effects. The induced-vortex contributions have the superscript (3) whilst the quantity $\lambda_3(Z)Y$ is the vortex-streamwise shear that arises through feedback from the buffer deck. We note that two streamwise length scales are active: the triple-deck scale X, and the modulated scale $X = h^{-6/5}\bar{X}$, responsible for wave growth or decay and vortex variations. Hence $\partial_X \rightarrow \partial_X + h^{6/5}\partial_{\bar{X}}$, effectively. Finally,we expand λ as $1 + h^{6/5}\lambda_1 + \cdots$, where λ_1 is real; this is possible provided the lower deck quantities adjust to accommodate the local variation of the skin-friction (Smith and Burggraf 1985).

We now substitute the above expansions into (3.1a-e) to obtain

$$i(\alpha Y - \Omega)\tilde{u}_{1n} + \tilde{v}_{1n} = -i\alpha\tilde{p}_{1n} + \tilde{u}_{1nYY}, \tag{3.3a}$$

$$i(\alpha Y - \Omega)\tilde{w}_{1n} = -\frac{i}{2}\beta_n\tilde{p}_{1n} + \tilde{w}_{1nYY}, \tag{3.3b}$$

$$i\alpha\tilde{u}_{1n} + \tilde{v}_{1nY} + \frac{i}{2}\beta_n\tilde{w}_{1n} = 0; \tag{3.3c}$$

$$i(\alpha Y - \Omega)\tilde{u}_{a1n} + Y\tilde{u}_{1n\bar{X}} + i\alpha\lambda_1 Y\tilde{u}_{1n} + i\alpha\left\{\begin{array}{l}\lambda_{33}\tilde{u}_{12}\\ -\lambda_{33}^*\tilde{u}_{11}\end{array}\right\} + \tilde{v}_{a1n}$$

$$+\tilde{v}_{1n}\lambda_1 + \left\{\begin{array}{l}\lambda_{33}\tilde{v}_{12}\\ \lambda_{33}^*\tilde{v}_{11}\end{array}\right\} + \frac{i}{2}(\beta_1 - \beta_2)\left\{\begin{array}{l}\lambda_{33}\tilde{w}_{12}\\ -\lambda_{33}^*\tilde{w}_{11}\end{array}\right\} = -i\alpha\tilde{p}_{a1n} - \tilde{p}_{1n\bar{X}} + \tilde{u}_{a1nYY}, \tag{3.4a}$$

$$i(\alpha Y - \Omega)\tilde{w}_{a1n} + Y\tilde{w}_{1n\bar{X}} + i\alpha\lambda_1 Y\tilde{w}_{1n} + \left\{\begin{array}{l}\lambda_{33}\tilde{w}_{12}\\ -\lambda_{33}^*\tilde{w}_{11}\end{array}\right\} = -\frac{i}{2}\beta_n\tilde{p}_{a1n} + \tilde{w}_{a1nYY}, \tag{3.4b}$$

$$i\alpha\tilde{u}_{a1n} + \tilde{u}_{1n\bar{X}} + \tilde{v}_{a1nY} + \frac{i}{2}\beta_n\tilde{w}_{a1n} = 0; \tag{3.4c}$$

$$\tilde{v}_{11}\tilde{u}_{12Y}^* + \tilde{v}_{12}^*\tilde{u}_{11Y} + \tilde{v}_{33} + \frac{i}{2}(\beta_1\tilde{u}_{11}\tilde{w}_{12}^* - \beta_2\tilde{u}_{12}^*\tilde{w}_{11}) = \tilde{u}_{33YY}, \tag{3.5a}$$

$$i\alpha(\tilde{u}_{12}^*\tilde{w}_{11} - \tilde{u}_{11}\tilde{w}_{12}^*) + \tilde{v}_{11}\tilde{w}_{12Y}^* + \tilde{v}_{12}^*\tilde{w}_{11Y} + \frac{i}{2}(\beta_1 - \beta_2)\tilde{w}_{11}\tilde{w}_{12}^* = \tilde{w}_{33YY}, \tag{3.5b}$$

$$\tilde{v}_{33Y} + \frac{i}{2}(\beta_1 - \beta_2)\tilde{w}_{33} = 0; \tag{3.5c}$$

for the main TS,forced TS and vortex flow,respectively,where the associated pressures $\tilde{p}_{1n}, \tilde{p}_{a1n}, \tilde{p}_{33}$ are independent of Y, and zero speed is observed at the wall. Here we have employed the TS- and vortex- properties described in the Introduction,that is

$$\tilde{u}^{(1)} = \tilde{u}_{11}(\bar{X}, Y)E_1 + \tilde{u}_{12}(\bar{X}, Y)E_2 + c.c., \tag{3.6a}$$

$$\tilde{u}_a^{(1)} = \tilde{u}_{a11}(\bar{X}, Y)E_1 + \tilde{u}_{a12}(\bar{X}, Y)E_2 + c.c., \tag{3.6b}$$

$$\tilde{u}^{(3)} = \tilde{u}_{33}(\bar{X}, Y)E_3 + c.c., \tag{3.6c}$$

etc.,and equated coefficients of E_1, E_2 for the TS equations and the coefficients of E_3 for the vortex equations. We return to these equations later after we have established some necessary results from the buffer,main and upper decks. For now we observe the far-field properties

$$\tilde{u}_{1n} \sim 1, \tilde{v}_{1n} \sim Y, \tilde{w}_{1n} \sim Y^{-1}, \tilde{p}_{1n} \sim 1; \tag{3.7a-d}$$

$$\tilde{u}_{a1n} \sim 1, \tilde{v}_{a1n} \sim Y, \tilde{w}_{a1n} \sim Y^{-1}, \tilde{p}_{a1n} \sim 1; \tag{3.8a-d}$$

$$\tilde{u}_{33} \sim Y^3 \ln Y, \tilde{v}_{33} \sim Y \ln Y, \tilde{w}_{33} \sim \ln Y, \tilde{p}_{33} \sim 1; \tag{3.9a-d}$$

as $Y \to \infty$. The logarithmic results in (3.9a-d) rely on neutrality of the waves and on imposing a vortex-spanwise-shear constraint at the wall,namely

$$\tilde{w}_{33Y}(0) = \int_0^\infty F(Y)dY, \tag{3.10}$$

where F is the wave-forcing on the left-hand side of (3.5b).

3.3 The buffer deck

This region is needed to adjust the vortex flow to the outer constraint in (2.1e) above. We write the velocity and pressure as

$$\tilde{u} = h^{-2/5}\hat{y} + h^{4/5}(\hat{u}^{(3)} + \lambda_1\hat{y}) + \cdots + hL\hat{u}^{(1)} + \cdots + h^{11/5}L\hat{u}_a^{(1)} + \cdots, \tag{3.11a}$$

$$\tilde{v} = h^{3/5}L\hat{v}^{(1)} + \cdots + h^{8/5}\hat{v}^{(3)} + \cdots + h^{9/5}L\hat{v}_a^{(1)} + \cdots, \tag{3.11b}$$

$$\tilde{w} = h^{7/5}L\hat{w}^{(1)} + \cdots + h^2\hat{w}^{(3)} + h^{13/5}L\hat{w}_a^{(1)} + \cdots, \tag{3.11c}$$

$$\tilde{p} = hL\hat{p}^{(1)} + \cdots + h^{11/5}L\hat{p}_a^{(1)} + \cdots + h^{16/5}\hat{p}^{(3)} + \cdots, \tag{3.11d}$$

where $(\tilde{u}, \tilde{v}, \tilde{w}, \tilde{p})$ satisfy (3.1a-d),but with $Y = h^{-2/5}\hat{y}$, where $\hat{y}$ is $O(1)$.

Thus we generate the sets of equations

$$\hat{y}\hat{u}_X^{(1)} + \hat{v}^{(1)} = 0, \tag{3.12a}$$

$$\hat{y}\hat{w}_X^{(1)} = -\hat{p}_Z^{(1)}, \tag{3.12b}$$

$$\hat{u}_x^{(1)} + \hat{v}_{\hat{y}}^{(1)} = 0; \tag{3.12c}$$

$$\hat{y}(\hat{u}_{aX}^{(1)} + \hat{u}_X^{(1)}) + (\hat{u}^{(3)} + \lambda_1\hat{y})\hat{u}_X^{(1)} + \hat{v}^{(1)}(\hat{u}_{\hat{y}}^{(3)} + \lambda_1) + \hat{v}_a^{(1)} = 0, \tag{3.13a}$$

$$\hat{y}(\hat{w}_{aX}^{(1)} + \hat{w}_X^{(1)}) + (\hat{u}^{(3)} + \lambda_1\hat{y})\hat{w}_X^{(1)} = 0, \tag{3.13b}$$

$$\hat{u}_{aX}^{(1)} + \hat{u}_X^{(1)} + \hat{v}_{a\hat{y}}^{(1)} = 0; \tag{3.13c}$$

$$\hat{y}\hat{u}_X^{(3)} + \hat{v}^{(3)} = \hat{u}_{\hat{y}\hat{y}}^{(3)}, \tag{3.14a}$$

$$\hat{y}\hat{w}_X^{(3)} = \hat{w}_{\hat{y}\hat{y}}^{(3)}, \tag{3.14b}$$

$$\hat{u}_X^{(3)} + \hat{v}_{\hat{y}}^{(3)} + \hat{w}_Z^{(3)} = 0; \tag{3.14c}$$

for the main TS,the forced TS and the vortex flows,in turn,where again the corresponding pressures are independent of the normal scale. Each set of equations is to be solved subject to the external displacement condition (2.1e) where,for each of the above systems,this reduces to

$$(\hat{u}^{(1)}, \hat{u}_a^{(1)}, \hat{u}^{(3)}) \to (\bar{A}^{(1)}(\bar{X}), \bar{A}_a^{(1)}(\bar{X}), \hat{A}^{(3)}(\bar{X})), \tag{3.15a-c}$$

$$(\hat{w}^{(1)}, \hat{w}_a^{(1)}, \hat{w}^{(3)}) \sim \hat{y}^{-1}, \tag{3.15d-f}$$

as $\hat{y} \to \infty$. Here the displacement decrement A has the expansion

$$A = h^{4/5}\bar{A}^{(3)} + hL\bar{A}^{(1)} + \cdots + h^{11/5}\bar{A}_a^{(1)} + \cdots. \tag{3.16}$$

For the main TS part we find simple slip-effect solutions hold:

$$\hat{u}^{(1)} = \bar{A}^{(1)}, \qquad \hat{v}^{(1)} = -\hat{y}\bar{A}_X^{(1)}, \tag{3.17a,b}$$

$$\hat{w}^{(1)} = \left\{-\frac{\beta_1\tilde{p}_{11}}{2\alpha\hat{y}}E_1 + \frac{\beta_2\tilde{p}_{12}}{2\alpha\hat{y}}E_2\right\} + c.c., \qquad \hat{p}^{(1)} = \tilde{p}^{(1)}, \tag{3.17c,d}$$

where

$$\bar{A}^{(1)} \equiv \bar{A}_{11}(\bar{X})E_1 + \bar{A}_{12}(\bar{X})E_2 + c.c. \tag{3.18}$$

Consistent lower-deck matching is required as $\hat{y} \to 0^+$, suggesting that

$$\tilde{u}^{(1)} \to \bar{A}^{(1)} \qquad \text{as } Y \to \infty \tag{3.19}$$

in the lower deck.

Next,(3.13a-c),solved in conjunction with (3.15b,e),yields in particular

$$\hat{u}_a^{(1)} = \hat{u}_{\hat{y}}^{(3)}\bar{A}^{(1)} + \bar{A}_a^{(1)}, \tag{3.20a}$$

$$\hat{v}_a^{(1)} = -\hat{y}(\bar{A}_{\bar{X}}^{(1)} + \bar{A}_{aX}^{(1)}) - \hat{u}^{(3)}\bar{A}^{(1)}, \tag{3.20b}$$

where

$$\bar{A}_a^{(1)} \equiv \bar{A}_{a11}(\bar{X})E_1 + \bar{A}_{a12}(\bar{X})E_2 + c.c. \tag{3.21}$$

Compatible matching with the lower deck solution will be guaranteed so long as

$$\tilde{u}_a^{(1)} \to \lambda_3\bar{A}^{(1)} + \bar{A}_a^{(1)} \qquad \text{as } Y \to \infty \tag{3.22}$$

in the lower deck.

The equations for the vortex,(3.14a-c),are partial-differential being dependent on $\hat{y}$ and $\bar{X}$. They are insoluble at present since they depend on the unknown wave-pressure terms $\tilde{p}_{11}, \tilde{p}_{12}$, via a slip condition on $\hat{w}^{(3)}$ at the buffer-deck wall. Therefore,we must determine the dominant wave variations over the longer scale $\bar{X}$, and this requires us to solve the pressure-displacement law (2.1f) for both the leading and forced TS waves,and subsequently coupling the results with each corresponding problem in the lower deck. Since the vortex pressure is mainly passive here,we need not concern ourselves with the vortex motion beyond this layer.

3.4 Pressure-displacement relations

An alternative to solving the Cauchy-Hilbert integral (2.1f) directly is to consider the Laplacian equation and associated boundary conditions from which the integral was derived,namely

$$\Big(\frac{\partial^2}{\partial X^2}+\frac{\partial^2}{\partial y'^2}+\frac{\partial^2}{\partial Z^2}\Big)p'=0, \tag{3.23a}$$

with

$$p'\to 0 \qquad \text{as } y'\to\infty, \tag{3.23b}$$

$$p'\to\bar{p}, \qquad p'_{y'}\to(u_e\partial_X+w_e\partial_Z)^2\bar{A} \qquad \text{as } y'\to 0^+. \tag{3.23c,d}$$

Here $y'(\equiv Re^{3/8}y)$ is the scaled upper deck transverse coordinate, and the pressure p' has the splitting

$$p'=hLp'^{(1)}+\cdots+h^{11/5}Lp'^{(1)}_a+\cdots \tag{3.24}$$

where

$$p'^{(1)}=p'_{11}(\bar{X},y')E_1+p'_{12}(\bar{X},y')E_2+c.c.,$$
$$p'^{(1)}_a=p'_{11}(\bar{X},y')E_1+p'_{12}(\bar{X},y')E_2+c.c.$$

Insertion of (3.24) into (3.23a-d) gives

$$\frac{\partial^2 p'_{1n}}{\partial y'^2}-(\alpha^2+\beta_n^2/4)p'_{1n}=0, \tag{3.25a}$$

with

$$p'_{1n}\to 0 \qquad \text{as } y'\to\infty, \tag{3.25b}$$

$$p'_{1n}\to\tilde{p}_{1n}, \qquad p'_{1ny'}\to-(\alpha u_e+\beta_n w_e/2)^2\bar{A}_{1n} \qquad \text{as } y'\to 0^+, \tag{3.25c,d}$$

for $n=1,2$ to leading order. This yields

$$(\alpha^2+\beta_n^2/4)^{1/2}\tilde{p}_{1n}(\bar{X})=(\alpha+\beta_n w_e/2)^2\bar{A}_{1n}(\bar{X}), \tag{3.26a,b}$$

for $n=1,2$ where,without loss of generality, $u_e=1$.

The second level equations are

$$\frac{\partial^2 p'_{a1n}}{\partial y'^2}-(\alpha^2+\beta_n^2/4)p'_{a1n}=-2i\alpha p'_{1n\bar{X}}, \tag{3.27a}$$

with

$$p'_{a1n} \to 0 \qquad \text{as } y' \to \infty, \tag{3.27b}$$

$$p'_{a1n} \to \tilde{p}_{a1n} \qquad \text{as } y' \to 0^+, \tag{3.27c}$$

$$p'_{a1ny'} \to -(\alpha + \beta_n w_e/2)^2 \bar{A}_{1n} + 2i(\alpha + \beta_n w_e/2)\bar{A}_{1n\bar{X}}, \qquad \text{as } y' \to 0^+, \tag{3.27d}$$

for $n = 1, 2$ which we note is absent of any vortex forcing and therefore linear. In fact only the slow streamwise modulation of the main waves serves to drive the secondary waves. The solution of (3.27a-d) is

$$(\alpha^2 + \beta_n^2/4)^{1/2}\tilde{p}_{a1n}(\bar{X}) = (\alpha + \beta_n w_e/2)^2 \bar{A}_{a1n}(\bar{X}) - 2i(\alpha + \beta_n w_e/2)\bar{A}_{1n\bar{X}} + \frac{i\alpha(\alpha + \beta_n w_e/2)^2}{(\alpha^2 + \beta_n^2/4)}\bar{A}_{1n\bar{X}}, \tag{3.28a,b}$$

for $n = 1, 2$.

3.5 Neutral eigenrelations and pressure-amplitude equations

Having established the necessary upper-deck displacement laws,we now return to the lower deck and solve the leading TS and forced TS systems of equations therein, together with (3.26a,b),(3.28a,b) above. So for the leading waves we have

$$i(\alpha Y - \Omega)\tilde{u}_{1n} + \tilde{v}_{1n} = -i\alpha\tilde{p}_{1n} + \tilde{u}_{1nYY}, \tag{3.29a}$$

$$i(\alpha Y - \Omega)\tilde{w}_{1n} = -\frac{i}{2}\beta_{1n}\tilde{p}_{1n} + \tilde{w}_{1nYY}, \tag{3.29b}$$

$$i\alpha\tilde{u}_{1n} + \tilde{v}_{1nY} + \frac{i}{2}\beta_n\tilde{w}_{1n} = 0, \tag{3.29c}$$

with

$$\tilde{u}_{1n} = \tilde{v}_{1n} = \tilde{w}_{1n} = 0 \qquad \text{at } Y = 0 \tag{3.29d}$$

$$\tilde{u}_{1n} \sim \bar{A}_{1n}, \quad \tilde{w}_{1n} \sim Y^{-1} \qquad \text{as } Y \to \infty \tag{3.29e}$$

and

$$(\alpha^2 + \beta_n^2/4)^{1/2}\tilde{p}_{1n} = (\alpha + \beta_n w_e/2)^2 \bar{A}_{1n}, \tag{3.29f}$$

for $n = 1, 2$. From this we can deduce the dispersion relations

$$\alpha^2 \frac{Ai'(\xi_0)}{\kappa} = (i\alpha)^{1/3}(\alpha^2 + \beta_n^2/4)^{1/2}(\alpha + \beta_n w_e/2)^2, \tag{3.30a,b}$$

for $n = 1, 2$, where

$$\xi_0 \equiv -\frac{i^{1/3}\Omega}{\alpha^{2/3}}, \qquad \kappa \equiv \int_{\xi_0}^{i^{1/3}\infty} Ai(s)ds,$$

and Ai is the Airy function. The neutrality of the waves implies the values

$$\xi_0 = -d_1 i^{1/3}, \frac{Ai'(\xi_0)}{\kappa} = \frac{d_1}{d_2} i^{1/3},$$

where $d_1 \approx 2.3, d_2 \approx 2.3$, (Lin 1955,Smith 1979,Drazin and Reid 1981), so that (3.30a,b) become

$$\alpha^{5/3}(d_1/d_2) = (\alpha^2 + \beta_n^2/4)^{1/2}(\alpha + \beta_n w_e/2)^2, \qquad (3.31a,b)$$

for $n = 1, 2$. Notably the presence of cross-flow precludes any symmetry in the $\alpha - \beta$ plane,i.e. $\beta_1 = -\beta_2$ is impossible for any streamwise wavenumber unlike the instance of zero cross-flow where perfect symmetry occurs in the $\alpha-$ axis.

For the forced TS waves the governing equations are

$$i(\alpha Y - \Omega)\tilde{u}_{a1n} + Y\tilde{u}_{1n\bar{X}} + i\alpha\lambda_1 Y\tilde{u}_{1n} + i\alpha \left\{ \begin{array}{c} \lambda_{33}\tilde{u}_{12} \\ -\lambda_{33}^*\tilde{u}_{11} \end{array} \right\} + \tilde{v}_{a1n} + \tilde{v}_{1n}\lambda_1$$

$$+ \left\{ \begin{array}{c} \lambda_{33}\tilde{v}_{12} \\ \lambda_{33}^*\tilde{v}_{11} \end{array} \right\} + \frac{i}{2}(\beta_1 - \beta_2) \left\{ \begin{array}{c} \lambda_{33}\tilde{w}_{12} \\ -\lambda_{33}^*\tilde{w}_{11} \end{array} \right\} = -i\alpha\tilde{p}_{a1n} - \tilde{p}_{1n\bar{X}} + \tilde{u}_{a1nYY}, \qquad (3.32a)$$

$$i(\alpha Y - \Omega)\tilde{w}_{a1n} + Y\tilde{w}_{1n\bar{X}} + i\alpha\lambda_1 Y\tilde{w}_{1n} + \left\{ \begin{array}{c} \lambda_{33}\tilde{w}_{12} \\ -\lambda_{33}^*\tilde{w}_{11} \end{array} \right\} = -\frac{i}{2}\beta_n\tilde{p}_{a1n} + \tilde{w}_{a1nYY}, \qquad (3.32b)$$

$$i\alpha\tilde{u}_{a1n} + \tilde{u}_{1n\bar{X}} + \tilde{v}_{a1nY} + \frac{i}{2}\beta_n\tilde{w}_{a1n} = 0, \qquad (3.32c)$$

with

$$\tilde{u}_{a1n} = \tilde{v}_{a1n} = \tilde{w}_{a1n} = 0 \qquad \text{at } Y = 0, \qquad (3.32d)$$

$$\tilde{u}_{a1n} \sim \left\{ \begin{array}{c} \lambda_{33}\bar{A}_{12} \\ \lambda_{33}^*\bar{A}_{11} \end{array} \right\} + \bar{A}_{a1n}, \tilde{w}_{a1n} \sim Y^{-1} \qquad \text{as } Y \to \infty, \qquad (3.32e)$$

and

$$(\alpha^2 + \beta_n^2/4)^{1/2}\tilde{p}_{a1n} = (\alpha + \beta_n w_e/2)^2 \bar{A}_{a1n}(\bar{X}) - 2i(\alpha + \beta_n w_e/2)\bar{A}_{1n\bar{X}} + \frac{i\alpha(\alpha + \beta_n w_e/2)^2}{(\alpha^2 + \beta_n^2/4)}\bar{A}_{1n\bar{X}}, \qquad (3.32f)$$

for $n = 1, 2$. After much working,we deduce the pressure-amplitude equations

$$a_1' \frac{d\tilde{p}_{11}}{d\bar{X}} + b_1' \lambda_1 \tilde{p}_{11} + c_1 \lambda_{33} \tilde{p}_{12} = 0, \tag{3.33a}$$

$$a_2' \frac{d\tilde{p}_{12}}{d\bar{X}} + b_1' \lambda_1 \tilde{p}_{12} + c_2' \lambda_{33}^* \tilde{p}_{11} = 0, \tag{3.33b}$$

hold,where

$$a_n' = \frac{2B_n \tau_n^2 \xi_0 r_1 D}{3\alpha^3 \Delta^{2/3}} - iB_n^{-1/2}\Big(\Big[\frac{-2}{3} + \frac{2\alpha}{\tau_n}\Big] + \frac{\beta_n^2}{\alpha^2}\Big[-\frac{5}{12} + \frac{\alpha}{2\tau_n}\Big]\Big), \tag{3.34a}$$

$$b_n' = -\frac{2B_n \tau_n^2 \xi_0 r_1 D}{3\alpha\Delta^{5/3}} - \frac{5B_n^{1/2}}{3\alpha}, \tag{3.34b}$$

$$\begin{aligned} c_n' = iD\xi_0 \Delta^{-2/3}\Big(\frac{2(B_1B_2)^{1/2}\tau_n^6 r_1}{3\alpha^2 \tau_1^2 \tau_2^2} - \frac{\sigma_n \tau_n^2 \beta_1 \beta_2 r_2}{8\alpha^2}\Big) \\ - \alpha^{-1} B_n^{-1/2}\Big(\frac{5\tau_n^4 (B_1B_2)^{1/2}}{3\tau_1^2\tau_2^2} + \frac{3\sigma_n \beta_1 \beta_2}{8}\Big), \end{aligned} \tag{3.34c}$$

for $n = 1, 2$. Here $B_n = (\alpha^2 + \beta_n^2/4), \tau_n = (\alpha + \beta_n w_e/2), \sigma_n = (1 - \beta_1\beta_2/\beta_n^2), D = 1 + \kappa\xi_0/Ai(\xi_0), \Delta = i\alpha, r_1 = Ai(\xi_0)/Ai'(\xi_0), r_2 = \kappa/Ai(\xi_0)$ and ξ_0, κ are as defined above.

The pressure-amplitude equations illustrate that the growth rate of each wave is affected by the basic-flow shear correction (λ_1) and the buffer-deck vortex- streamwise shear (λ_{33}); the cross-flow influence is reflected by the interaction coefficients a_n', b_n', c_n'. We are prevented from solving the amplitude equations as they stand because the vortex (and hence λ_{33}) has implicit dependence on the wave pressures $\tilde{p}_{11}, \tilde{p}_{12}$, as mentioned in Section 3.3 above. Instead we must solve the wave- and vortex-equations interactively,although firstly we need to ascertain the boundary conditions for the vortex at the buffer-deck wall.

We know from above that,in the lower deck,wave-inertial forcing provokes logarithmic growth in the vortex-spanwise velocity component. A more detailed evaluation comes from substituting the asymptotic properties

$$\tilde{u}_{1n} = \bar{A}_{1n} + \Big(\frac{\beta_n^2}{4\alpha^2}\Big)Y^{-1} + \cdots, \tag{3.35a}$$

$$\tilde{v}_{1n} = -(i\alpha\bar{A}_{1n})Y + \Big[i\Omega\bar{A}_{1n} - i\alpha\Big(1 + \frac{\beta_n^2}{4\alpha^2}\Big)\tilde{p}_{1n}\Big] + \cdots, \tag{3.35b}$$

$$\tilde{w}_{1n} = -\Big(\frac{\beta_n}{2\alpha}\tilde{p}_{1n}\Big)Y^{-1} + \cdots, \tag{3.35c}$$

of the leading waves into the lower-deck spanwise-vortex equation (3.5b) above. It is found that

$$\tilde{w}_{33} \sim -iK\tilde{p}_{11}\tilde{p}_{12}^* \ln Y, \qquad \text{for } Y \gg 1, \tag{3.36}$$

where

$$K = \frac{1}{2}(\beta_1 - \beta_2)\Big(1 + \frac{\beta_1\beta_2}{4\alpha^2}\Big). \tag{3.37}$$

The logarithmic growth in $\tilde{w}_{33}$ is known to induce the other properties $\tilde{u}_{33} \sim Y^3 \ln Y, \tilde{v}_{33} \sim Y \ln Y$ as $Y \to \infty$, in the lower deck. Therefore,the inner constraints for the vortex in the buffer deck are

$$\hat{u}_{33} \to 0, \hat{v}_{33} \to 0, \hat{w}_{33} \to -iK\tilde{p}_{11}\tilde{p}_{12}^* \qquad \text{as } \hat{y} \to 0^+. \tag{3.38a-c}$$

3.6 The interaction equations

In summary,the nonlinear vortex/TS interaction is embodied in the equations

$$\hat{y}U_{\bar{X}} + V = U_{\hat{y}\hat{y}}, \tag{3.39a}$$

$$\hat{y}W_{\bar{X}} = W_{\hat{y}\hat{y}}, \tag{3.39b}$$

$$U_{\bar{X}} + V_{\hat{y}} + \frac{i}{2}(\beta_1 - \beta_2)W = 0, \tag{3.39c}$$

with

$$U(\bar{X}, \infty) = A, \qquad W(\bar{X}, \infty) = 0, \tag{3.39d}$$

$$U(\bar{X}, 0) = 0, \qquad W(\bar{X}, 0) = -iKP_{11}P_{12}^*, \tag{3.39e}$$

and

$$\frac{dP_{11}}{d\bar{X}} + b_1\lambda_1 P_{11} + c_1\lambda_{33}P_{12} = 0, \tag{3.39f}$$

$$\frac{dP_{12}}{d\bar{X}} + b_2\lambda_1 P_{12} + c_2\lambda_{33}^* P_{11} = 0, \tag{3.39g}$$

where $\hat{u}_{33}, \hat{v}_{33}, \hat{w}_{33}, \bar{A}_{33}, \tilde{p}_{11}, \tilde{p}_{12}$ have,in turn,been replaced by $U, V, W, A, P_{11}, P_{12}$, and $b_n = b_n'/a_n', c_n = c_n'/a_n' (n = 1, 2)$. Defining $\tau = U_{\hat{y}}$ (so that $\tau(\bar{X}, 0) = \lambda_{33}(\bar{X})$),(3.39a-c) simplify to

$$\tau_{\hat{y}\hat{y}} - \hat{y}\tau_{\bar{X}} = -\frac{i}{2}(\beta_1 - \beta_2)W, \tag{3.40a}$$

$$W_{\hat{y}\hat{y}} - \hat{y}W_{\bar{X}} = 0, \tag{3.40b}$$

with

$$\tau(\bar{X}, \infty) = W(\bar{X}, \infty) = 0, \tag{3.40c}$$

$$\tau_{\hat{y}}(\bar{X}, 0) = 0, \quad W(\bar{X}, 0) = -iKP_{11}P_{12}^*. \tag{3.40d}$$

In principle,we may solve (3.40a-d) collectively with (3.39f,g),given some prescribed input conditions in $\bar{X}$. Analogous equations to (3.39a-g),(3.40a-d) were obtained by Smith and Blennerhassett (1992) for zero cross-flow,where the authors corrected the original zero cross-flow "interaction equations" in Hall and Smith (1989) . In both papers,a partial-differential finite-scheme was applied directly to the vortex-wave equations.

It is possible to reduce the $\tau - W$ system above to an integral equation for λ_{33}, however,if we consider the special case of zero-input vortex flow, i.e. $W = \tau = 0$ at $\bar{X} = 0$ (without loss fo generality). We apply the Laplace transform in $\bar{X}$ to (3.40a-d) and obtain

$$\bar{W} = -\frac{iK\bar{P}}{Ai(0)} Ai(s^{1/3}\hat{y}), \tag{3.41a}$$

and

$$\bar{\tau} = \frac{K\bar{P}}{2Ai(0)}(\beta_1 - \beta_2)s^{-2/3} Ai(s^{1/3}\hat{y}), \tag{3.41b}$$

where

$$\bar{\tau}(s,\hat{y}) = \int_0^\infty \tau(\bar{X},\hat{y})e^{-s\bar{X}}d\bar{X}, \qquad W(s,\hat{y}) = \int_0^\infty W(\bar{X},\hat{y})e^{-s\bar{X}}d\bar{X},$$

$$\bar{P}(s) = \int_0^\infty P_{11}(\bar{X})P_{12}^*(\bar{X})e^{-s\bar{X}}d\bar{X}$$

are the Laplacian transforms of $\tau, W, P_{11}P_{12}^*$ respectively. Hence, (3.41b) evaluated at $\hat{y} = 0$ and inverted gives

$$\lambda_{33}(\bar{X}) = MK\tilde{\beta}\int_0^{\bar{X}} P_{11}(u)P_{12}^*(u)(\bar{X} - u)^{-1/3}du, \tag{3.42}$$

where $\tilde{\beta} \equiv (\beta_1 - \beta_2)/2, M \approx 0.54$. Then unifying (3.42) and (3.39f,g),and prescribing values for P_{11}, P_{12} at $\bar{X} = 0$, we can determine the flow solution for $\bar{X} > 0$. Numerically, our task is much easier, since we have eliminated one variable ($\hat{y}$) entirely and we do not therefore need to resort to the potentially difficult and computationally expensive two-variable finite-difference schemes. On the other hand,for non-zero vortex input the same Laplace transform scheme for (3.40a-d) would yield additional terms,generally triple integrals,on the right-hand-side of (3.42),and in this case the finite-difference scheme would possibly be the better choice.

For all the ensuing weakly nonlinear analysis,we concentrate on the case of zero-input vortices. Computations have been performed for a full 3D boundary layer, i.e. $w_e = O(1)$,and these are presented in the next section.

4. COMPUTATIONAL SOLUTIONS

We applied a predictor-corrector scheme of second-order accuracy to advance the wave pressures in distance and a trapezoidal rule to calculate the vortex-shear integral at each station. This procedure proved to be stable and accurate for suitably small step lengths. Interaction results were obtained for sample values of α and w_e and all starting at $\bar{X} = 0$ upstream of the neutral TS point. The input value for each wave pressure was fixed at 0.1. The basic-flow correction λ_1 was taken as positive and therefore normalised to +1.

Three main types of nonlinear behaviour are found to occur downstream and,in light of the numerical findings,we now address these analytically. Firstly,there is the situation (figures 2,5,8 and 9) where the flow solution develops an algebraic singularity at a finite position downsream,say as $\bar{X} \to \bar{X}_s$; the orders of magnitude suggest the scalings

$$P_{11} \sim \zeta^{-5/6} e^{i\phi_1(\zeta)} |\tilde{P}_{11}| + \cdots, \tag{4.1a}$$

$$P_{12} \sim \zeta^{-5/6} e^{i\phi_2(\zeta)} |\tilde{P}_{12}| + \cdots, \tag{4.1b}$$

$$\lambda_{33} \sim \zeta^{-1} e^{i[\phi_1(\zeta) - \phi_2(\zeta)]} \tilde{\lambda}_{33} + \cdots, \tag{4.1c}$$

where $\zeta \equiv (\bar{X}_s - \bar{X})$, and $0 < \zeta \ll 1$. Here the real-valued phase factors ϕ_1, ϕ_2 expand as

$$\phi_1 \sim \phi_{10} \ln \zeta + \phi_{11} + \phi_{12}\zeta + \cdots, \tag{4.2a}$$

$$\phi_2 \sim \phi_{20} \ln \zeta + \phi_{21} + \phi_{22}\zeta + \cdots, \tag{4.2b}$$

where $\phi_{10}, \phi_{11}, \phi_{12}, \phi_{20}, \phi_{21}, \phi_{22}, \cdots$ are unknown constants. The analysis produces the solvability conditions

$$K(c_{1r} - \delta_0 c_{1i}) < 0, \tag{4.3a}$$

$$K(c_{2r} - \delta_0 c_{2i}) < 0, \tag{4.3b}$$

where c_{1r}, c_{1i} denote the real and imaginary parts of c_1 in turn and likewise for the other interaction coefficients. Also $\delta_0 (\equiv \phi_{10} - \phi_{20})$, the dominant phase difference of the pressures,satisfies the cubic equation

$$a_3 \delta_0^3 + a_2 \delta_0^2 + a_1 \delta_0 + a_0 = 0, \tag{4.4}$$

where

$$a_3 = 6c_{1i}c_{2i}, \qquad a_2 = 11(c_{1i}c_{2r} - c_{1r}c_{2i}), \tag{4.5a,b}$$

$$a_1 = -2(8c_{1r}c_{2r} + c_{1i}c_{2i}), \qquad a_0 = 5(c_{1r}c_{2i} - c_{1i}c_{2r}). \tag{4.5c,d}$$

Secondly,there is the option of saturation where the nonlinear quantities develop the form

$$P_{11} \sim |\hat{P}_{11}| e^{i\theta_1 \bar{X}}, \qquad P_{12} \sim |\hat{P}_{12}| e^{i\theta_2 \bar{X}}, \tag{4.6a,b}$$

as $\bar{X} \to \infty$ (see figures 6 and 7). The analysis yields the criteria

$$\frac{K}{b_{1r}} \Re[e^{-i\pi/3} c_1] < 0, \frac{K}{b_{2r}} \Re[e^{i\pi/3} c_2] < 0, \tag{4.7a,b}$$

and

$$\Delta_0 \Big(= b_{1r} \frac{\Im[e^{-i\pi/3} c_1]}{\Re[e^{-i\pi/3} c_1]} - b_{2r} \frac{\Im[e^{i\pi/3} c_2]}{\Re[e^{i\pi/3} c_2]} - (b_{1i} - b_{2i}) \Big) > 0, \tag{4.7c}$$

where $\delta_0(\equiv \theta_1 - \theta_2)$ is the wave-pressure phase difference at the point of saturation,and $\Re, \Im$ denote the real and imaginary parts of their enclosed quantities,respectively.

Finally,there is the possibility that both waves will decay far downstream in an exponential manner under linear forces, i.e. acquire the form

$$P_{11} \sim |\bar{P}_{11}|e^{-b_1\bar{X}}, \qquad P_{12} \sim |\bar{P}_{12}|e^{-b_2\bar{X}} \tag{4.8a,b}$$

as $\bar{X} \to \infty$. This is clearly valid so long as

$$b_{1r} > 0, \qquad b_{2r} > 0. \tag{4.9a,b}$$

The vortex-shear decays in a much slower (algebraic) fashion because of its dependence on the history of the flow solution. Figures 3 and 4 illustrate this option.

The values of the wave angles and the cross-flow upon which the interaction coefficients depend generally determine which option will come into play downstream but no explicit constraints on these parameters have been deduced due to the complexity of the analysis. The numerical results do indicate however that an algebraic singularity only occurs if one of the modes is the "lower" branch cross- flow mode. (See Appendix B for a description of the modes and a summary of the linear neutral stability in the presence of cross-flow.)

5. FINAL COMMENTS

It has been shown in the preceding sections that significant interactions between two TS waves and an induced or incident vortex in a cross-flow boundary layer can lead to three types of behaviour downstream. An interesting point is that the results are very much in line with the related work on channel flows and boundary layers for zero cross-flow by Smith and Blennerhassett (1992). Firstly,the flow solution breaks down in an algebraic fashion at some finite position downstream. This points to the entry of a stronger and probably fully nonlinear stage more locally. Secondly,the flow solution may saturate far downstream, i.e. the flow quantities may asymptote to finite values as the streamwise coordinate becomes large. The computations show however that this second option is fairly infrequent and only seems to occur in a relatively small range of angles for each given cross-flow. This is considerably different from the Smith and Blennerhassett results,where most of the wave angles considered lead to the saturation case. Moreover,in their case the wave pressures decay to zero during saturation whereas the wave pressures in our case asymptote to non-zero values. Thirdly,the TS waves may decay exponentially at downstream infinity, essentially under linear forces,leaving pure vortex flow. (We note,however,that the magnitude of the vortex flow is smaller than in the previous region of full vortex/wave interaction,because in that region it decayed algebraically.) The numerical results tend to indicate that this third option happens only when both of the TS wave angles are greater than $-\arctan(w_e^{-1})$ to the $x-$direction (which we recall is the direction of the surface shear stress) . This,in turn,is possible only when the four-mode criterion, i.e. $w_e < 0.20$ approx.,as discussed in

Appendix B,is in effect,and neither mode is the "lower" branch cross-flow mode,whose angle is always less than $-\arctan(w_e^{-1})$ to the $x-$direction. In contrast,the first and second options seem to occur only when one of the modes is the "lower" branch cross-flow mode.

The neutral stability curve that stems from linear TS theory has been illustrated for the cases $w_e = 0, \quad 0 < w_e \ll 1$ and $w_e = O(1)$ in Appendix B. It can be seen that for all non zero cross-flow values the curve is open and unbounded, reflecting the property that the chosen wavenumber scales are not sufficiently large to capture the complete neutral curve, i.e. the "closure" of the curve. There the relevant streamwise scale in particular is $O(Re^{-3/7})$ instead of the triple-deck scale $O(Re^{-3/8})$, and corresponds to having significant vertical wave-acceleration entering the boundary layer and inducing a wave-pressure "jump" across the extremes of the boundary layer. If the jump is too large then the boundary layer cannot support neutral solutions (see Davis 1992). It is hoped that the weakly nonlinear theory will be extended to that regime in the future.

The current regime of triple-deck wavenumbers is of further interest because it enables comparisons to be made between the linear natures of the two cross-flow modes and the two regular 2D-type modes. More importantly,for cross-flow values less than 0.20,these modes co-exist,enabling us to consider the influence of each of the six possible pairs of modes on the weakly nonlinear interaction. In addition to the $O(1)$ computations presented above,some computations were also performed for the instance where the cross-flow parameter w_e is asymptotically small,based on the corresponding analysis in Davis (1992). In that analysis,it was shown that the two cross-flow modes expand in the form

$$\beta \sim (-2\alpha)w_e^{-1} \pm \hat{\beta}_1 w_e^{-1/2} + O(1) \qquad \text{as } w_e \to 0^+, \tag{5.1a,b}$$

where

$$\hat{\beta}_1 = 2(d_1/d_2)^{1/2}\alpha^{1/3}, \tag{5.2}$$

illustrating that these modes are nearly normal to the $x-$direction. Also it can be seen that the cross-flow influence remains despite the smallness of the cross-flow magnitude; this contrasts with the two regular modes which have the approximate 2D- boundary-layer forms

$$\beta \sim \pm\beta_0 + \bar{\beta}_1 w_e + O(w_e^2) \qquad \text{as } w_e \to 0^+. \tag{5.3a,b}$$

Here $\beta_0(> 0)$ is the "zero cross-flow" mode of Hall and Smith (1989) which satisfies the neutral equation

$$\frac{d_1}{d_2} = \alpha^{1/3}\Big(\alpha^2 + \frac{\beta_0^2}{4}\Big)^{1/2}, \tag{5.4}$$

and

$$\bar{\beta}_1 = -\frac{4}{\alpha}\Big(\alpha^2 + \frac{\beta_0^2}{4}\Big). \tag{5.5}$$

The computations for small cross-flow showed that the option of exponential decay would occur in the weakly nonlinear interactions unless one of the modes was the "lower" branch cross-flow mode. In the latter case the flow solution would blow up algebraically. These results are also largely consistent with the computations for O(1) cross-flows.

We conclude therefore that for cross-flow values less than 0.20 the nonlinear TS/ vortex interaction either undergoes an algebraic finite-distance blow-up or else the exponential-wave-decay/algebraic-vortex-decay option comes into play,depending entirely on whether or not the "lower" branch cross-flow mode is one of the two modes involved in the interaction,as discussed previously. For cross-flow values exceeding 0.20 however,the flow solution breaks up algebraically in all cases,except possibly in a small angle range where saturation occurs.

On a final matter,it is clear that this and probably the other vortex/TS-wave interaction structures possible (see also Section 1) tend to stay essentially unaltered by the additional presence of O(1) cross-flows, i.e. where the edge velocities u_e, w_e are comparable. By contrast,recent work by Davis (1992),Brown and Smith (1992) on the vortex/inviscid-wave interactions shows that even small amounts of cross-flow can substantially alter the original flow structures set up by Hall and Smith (1991) (for long scales),Smith,Brown and Brown (1992) (for short scales) for such interactions with zero cross-flow. There appears to be much to be clarified there.

APPENDIX A. EFFECTS OF NONPARALLELISM ON THE TS/VORTEX STRUCTURE

The global basic-flow velocity $(u, Re^{-1/2}v, w)$ has the expansion

$$u = \bar{u}(\bar{y}) + (x - x_0)u_b(\bar{y}) + \cdots, \tag{A1}$$

$$v = \bar{v}_b(\bar{y}) + \cdots, \tag{A2}$$

$$w = \bar{w}(\bar{y}) + (x - x_0)\bar{w}_b(\bar{y}) + \cdots, \tag{A3}$$

as $x \to x_0^+$ in the main deck. Nonparallelism becomes significant when the second terms in u, w and the first in v, start to drive the vortex-induced waves over the longer scale $\bar{X}$. Hence,we seek the balance

$$Re^{-3/8}h^{-6/5} \sim h^{6/5}, \qquad \text{i.e. } h \sim Re^{-5/32}.$$

The subsequent alteration to the interaction equations is the insertion of additional terms $(b_1\lambda_b\bar{X})P_{11}$ and $(b_2\lambda_b\bar{X})P_{12}$ in (3.39f,g) respectively,where $\lambda_b = \bar{u}_{b\bar{y}}(0)$. This may possibly lead to a substantial change in the development of the flow solution,especially if the nonlinear structure avoids breaking up after a finite distance downstream,but on the other hand nonparallelism may be passive. Much depends on the wave angles,the size of the cross-flow and the input conditions.

We observe that for $h \gg Re^{-5/32}$, nonparallelism is negligible. Thus with hindsight,the analysis of Section 3 is seen to be valid in the regime

$$Re^{-5/32} \ll h \ll 1.$$

APPENDIX B. EFFECTS OF CROSS-FLOW ON THE LINEAR TS STABILITY

The neutral stability curve that corresponds to the linear 3D dispersion relation

$$\alpha^{5/3}\left(\frac{d_1}{d_2}\right) = \left(\alpha^2 + \frac{\beta^2}{4}\right)^{1/2}\left(\alpha + \frac{\beta w_e}{2}\right)^2$$

is illustrated in Figure 1 for the cases $w_e = O(1), 0 < w_e \ll 1, w_e = 0$.

In particular,there are some striking differences between the last two curves: firstly the zero cross-flow curve is symmetric and extends across the entire $\beta-$range, whereas the small cross-flow curve remains asymmetric and has a finite cut-off value for some $\beta > 0$, above which no neutral solutions exist; secondly there is a vast difference between the respective maximum $\alpha-$values. When $w_e = 0$ this value is $(d_1/d_2)^{3/4} \approx 1$ and occurs when $\beta = 0$ (i.e. for 2D waves) but for all non- zero values of the cross-flow it is removed,in effect,to $\beta = -\infty$ and becomes infinite (pointing to the existence of important long-scale instabilities). Obviously the curves do not match uniformly (even though the regular "upper" branches coalesce) and an intermediate matching regime exists. Another feature of the small cross-flow curve distinct from the 2D curve is the presence of two "extra" modes,these being purely cross-flow generated. This points to the possibility of having six pairs of interactions for any given α lying inside the critical interval (0,1),(where we have given (d_1/d_2) the appromixate value of 1). This interval becomes thinner as cross-flow increases until eventually it vanishes for a critical cross-flow value,above which only the cross-flow modes exist. (This critical value has been determined to be $(\sqrt{24})^{-1}(\approx 0.20)$,where the "upper" branch has no maxima or minima.) Asymptotic solutions have been obtained for the weakly nonlinear interactions in the limit of small cross-flow (Davis 1992) .

REFERENCES

Aihara,Y.,1965, Bull. Aero. Res. Inst.,Tokyo Univ.,3, 195.

Aihara,Y.,Tani,I.,1969, J. Appl. Math. Phys.,20, 609.

Aihara,Y.,Koyama,H.,1981, Trans. Jap. Soc. Aero. Space Sci.,24, 78-94.

Aihara,Y.,Tomita,Y.,Ito,A.,1985, in "Laminar-Turbulent Transition," 447-454,V.V.Koslov ed.,Springer-Verlag.

Bennett,J.,Hall,P.,Smith,F.T.,1991. The strong nonlinear interaction of Tollmien-Schlichting waves and Taylor-Görtler vortices in curved channel flow. J. Fluid Mech. 223, 475-495.

Bippes,H.,Görtler,H.,1972. Dreidimensional Störungen in der Grenzschicht an einer konkaven Wand. Acta Mech.,14,251-267.

Bowles,R.,Smith,F.T.,1992.

Bowles,R.I.,Elliott,J.W.,Smith,F.T.,1992.

Brown,P.G.,Brown,S.N.,Smith,F.T.,1992.

Brown,S.N.,Smith,F.T.,1992.

Davis,D.A.R.,1992. Ph.D thesis,University of London,U.K.

Drazin,P.G.,Reid,W.H.,1981, Hydrodynamic Stability, Cambridge University Press.

Hall,P.,1986.

Hall,P.,Smith,F.T.,1988. The nonlinear interaction of Tollmien-Schlichting waves and Tayler-Görtler vortices in curved channel flows. Proc. R. Soc. Lond. A 417, 255-282.

Hall,P.,Smith,F.T.,1989. Nonlinear Tollmien-Schlichting/vortex interaction in boundary layers. Eur. J. Mech.,B8,179-205.

Hall,P.,Smith,F.T.,1991. On strongly nonlinear vortex/wave interactions in boundary-layer transition. J.Fluid Mech.,227,641-666.

Klebanoff,P.S.,Tidstrom,K.D.,1959. Evolution of amplified waves leading to transition in a boundary layer with zero pressure gradient. N.A.S.A. Tech. note,no. D-195.

Klebanoff,P.S.,Tidstrom,K.D.,Sargent,L.M.,1962. The three-dimensional nature of boundary layer instability. J. Fluid Mech.,12,1-34.

Lin,C.C.,1955, The Theory of Hydrodynamic Stability, Cambridge University Press.

Smith,F.T.,1979. On the non-parallel flow stability of the Blasius boundary layer. Proc. R. Soc. Lond.,A366,91-109.

Smith,F.T.,1988. Finite-time break-up can occur in any unsteady interacting boundary layer. Mathematika,35,256-273.

Smith,F.T.,Blennerhassett,P.,1992. Nonlinear interaction of oblique three- dimensional Tollmien-Schlichting waves and longitudinal vortices,in channel flows and boundary layers. Proc. R. Soc. Lond.,A436,585-602.

Smith,F.T.,Brown,S.N.,Brown,P.G.,1992.

Spalart,P.R.,Yang,K.-S.,1987. Numerical study of ribbon-induced transition in Blasius flow. J.Fluid Mech.,178,345-365.

Stewart,P.A.,Smith,F.T.,1987. Three-dimensional instabilities in steady and unsteady non- parallel boundary layers,including effects of Tollmien-Schlichting disturbances and cross flow. Proc. R. Soc. Lond.,A409,229-248.

Stewart,P.A.,Smith,F.T.,1992.

Stuart,J.T.,1963.

Tani,I.,Sakagami,J.,1962, in "Procs. of the Int. Council on Aeron. Sci.," 391-403,Third Congress,Stockholm,(Spartan,New York).

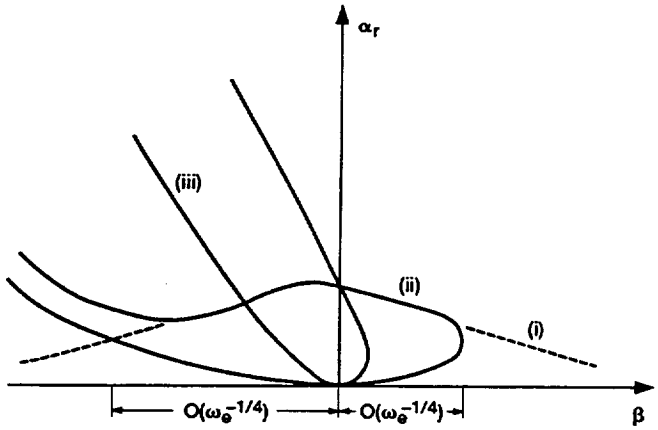

Figure 1.—Sketch of the linear TS neutral stability curves depicting the real part of α versus β for the cases (i) $\omega_e = 0$; (ii) $0 < \omega_e << 1$; and (iii) $\omega_e = O(1)$.

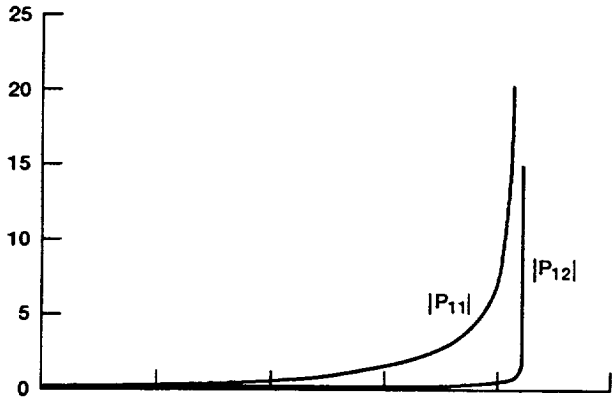

(a) TS pressure moduli ($|P_{11}|, P_{12}|$) versus $\bar{X}$.

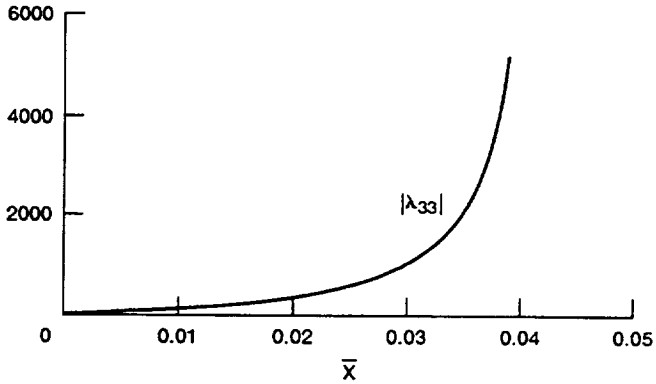

(b) Vortex shear modulus $|\lambda_{33}|$ versus $\bar{X}$.

Figure 2.—Nonlinear-interaction computed results. Wave angles at 86.42°, -89.59°. Cross-flow at 0.01, grid $\Delta\bar{X} = 10^{-5}$. Initial TS pressure moduli both 0.1, zero-input vortex flow.

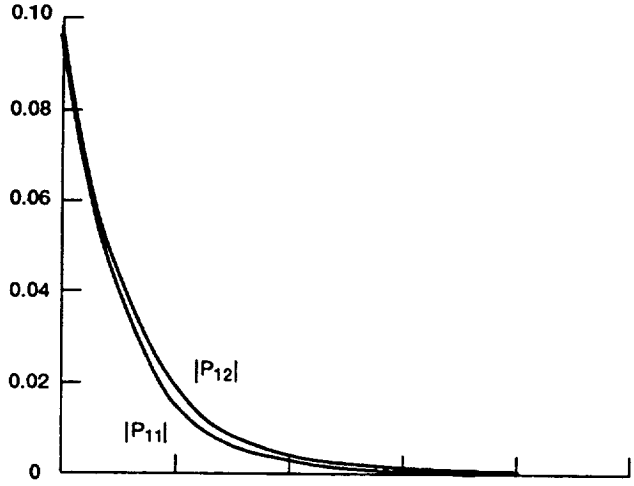

(a) $|P_{11}|, P_{12}|$ versus $\bar{X}$.

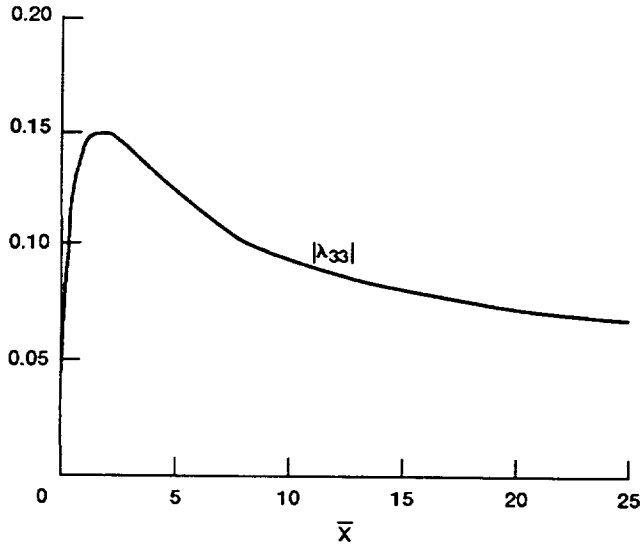

(b) $|\lambda_{33}|$ versus $\bar{X}$.

Figure 3.—Nonlinear-interaction computed results. Wave angles $\theta_1 = 65.56°$, $\theta_2 = -67.80°$. Cross-flow is 0.01, grid $\Delta\bar{X} = 5 \times 10^{-3}$. Initial |P11|, |P12| both 0.1, $|\lambda_{33}| = 0$.

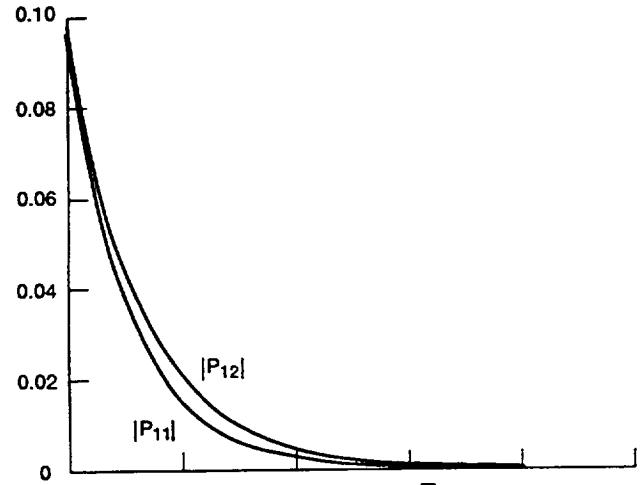

(a) $|P_{11}|, |P_{12}|$ versus $\bar{X}$.

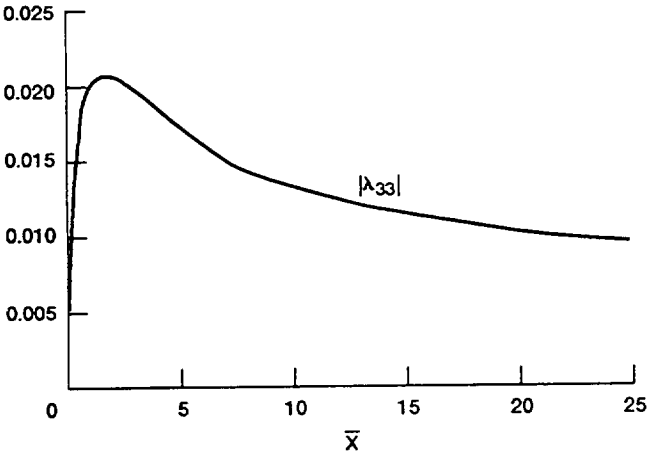

(b) $|\lambda_{33}|$ versus $\bar{X}$.

Figure 4.—Computational solutions of the nonlinear interaction. Wave angles $\theta_1 = 37.72°$, $\theta_2 = -65.36°$. Cross-flow is 0.1, grid $\Delta\bar{X} = 5 \times 10^{-3}$. Start |P11|, |P12| both 0.1, $|\lambda_{33}| = 0$.

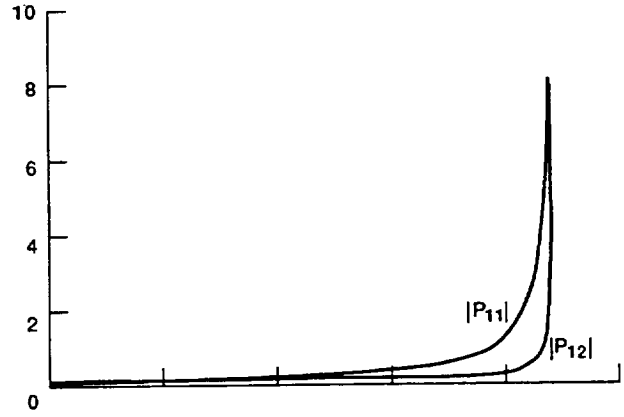

(a) $|P_{11}|, |P_{12}|$ versus $\bar{X}$.

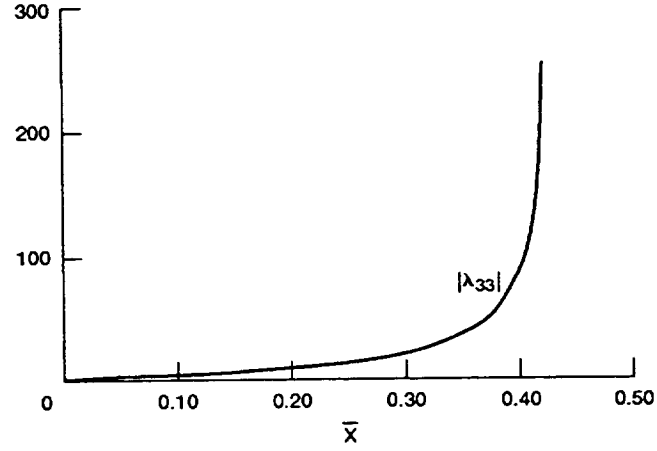

(b) $|\lambda_{33}|$ versus $\bar{X}$.

Figure 5.—Computational results of the nonlinear interaction. Wave angles at $\theta_1 = -76.31°$, $\theta_2 = -85.70°$. Cross-flow is 0.1, grid $\Delta\bar{X} = 10^{-4}$. Initial |P11|, |P12| both 0.1, $|\lambda_{33}| = 0$.

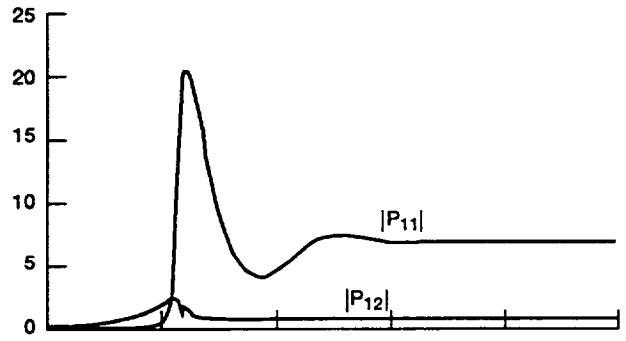

(a) $|P_{11}|, |P_{12}|$ versus $\bar{X}$.

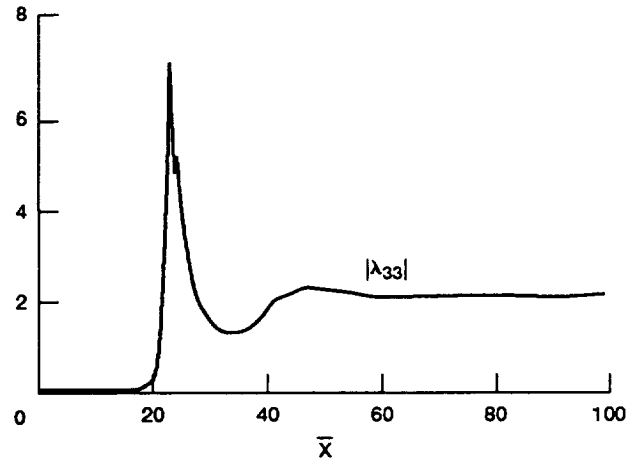

(b) $|\lambda_{33}|$ versus $\bar{X}$.

Figure 6.—Computational results. Wave angles $\theta_1 = 20.14°$, $\theta_2 = -71.85°$. Cross-flow is 1, grid $\Delta\bar{X} = 1.25 \times 10^{-2}$. Start |P11|, |P12| both 0.1, $|\lambda_{33}| = 0$.

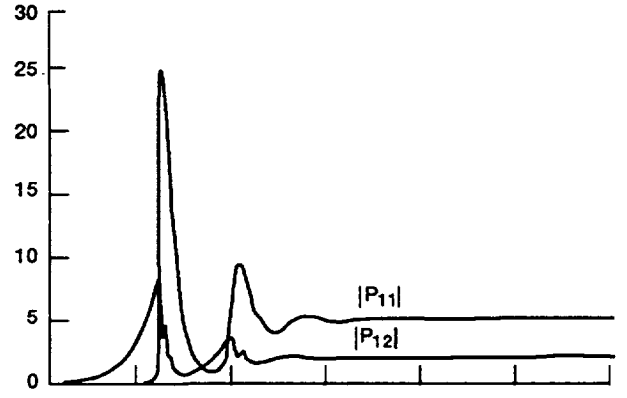

(a) $|P_{11}|, |P_{12}|$ versus $\bar{X}$.

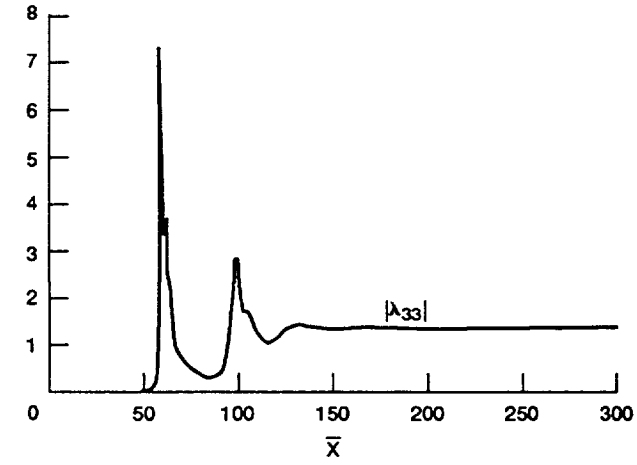

(b) $|\lambda_{33}|$ versus $\bar{X}$.

Figure 7.—Computational results. Wave angles $\theta_1 = 28.07°$, $\theta_2 = -53.47°$. Cross-flow is 2, grid $\Delta\bar{X} = 0.05$. Start |P11|, |P12| both 0.1, $|\lambda_{33}| = 0$.

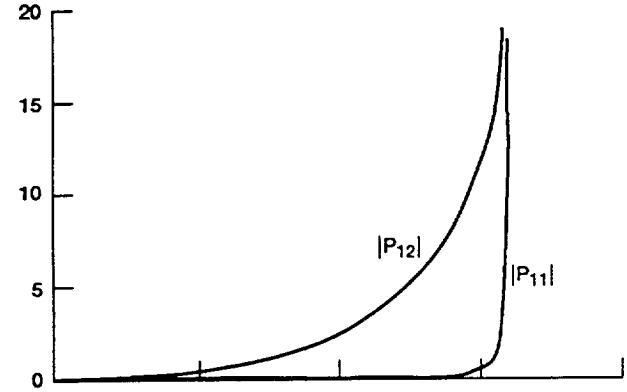

(a) $|P_{11}|, |P_{12}|$ versus $\overline{X}$.

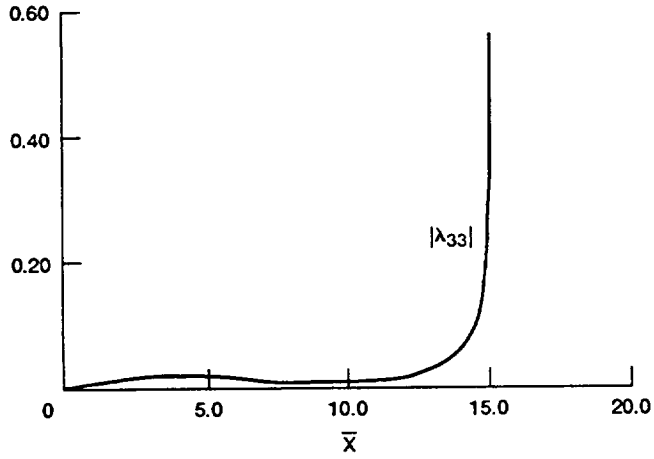

(b) $|\lambda_{33}|$ versus $\overline{X}$.

Figure 8.—Computational results. Wave angles $\theta_1 = -6.65°$, $\theta_2 = -39.81°$. Cross-flow is 2, grid $\Delta\overline{X} = 4 \times 10^{-3}$. Start |P11|,|P12| both 0.1,$|\lambda_{33}| = 0$.

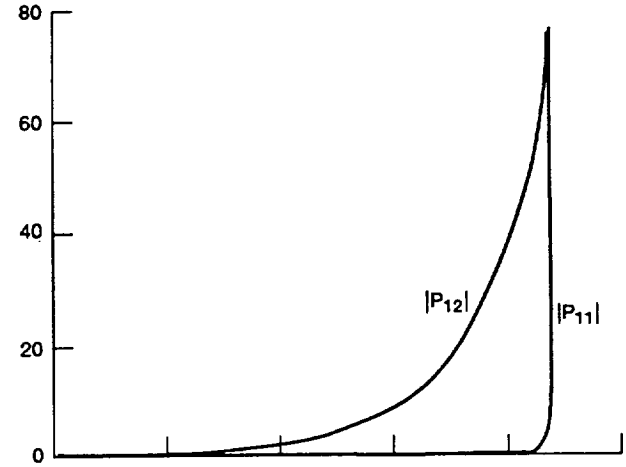

(a) $|P_{11}|, |P_{12}|$ versus $\overline{X}$.

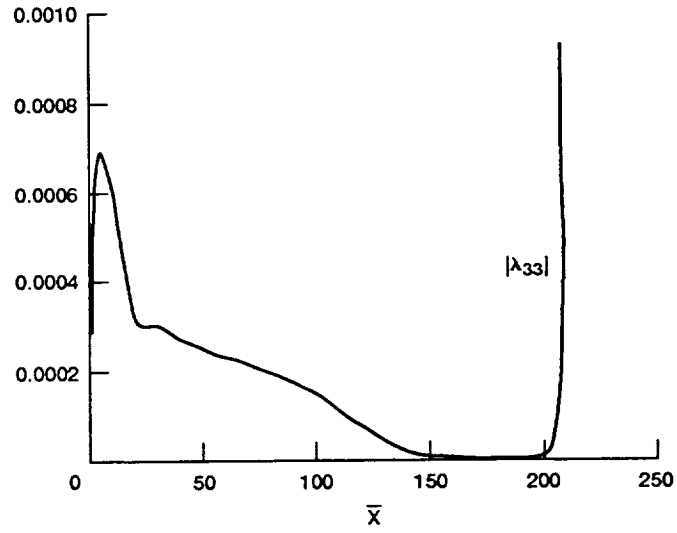

(b) $|\lambda_{33}|$ versus $\overline{X}$.

Figure 9.—Computational results. Wave angles $\theta_1 = 16.70°$, $\theta_2 = -33.42°$. Cross-flow is 5, grid $\Delta\overline{X} = 0.06$. Start |P11|,|P12| both 0.1,$|\lambda_{33}| = 0$.

REPORT DOCUMENTATION PAGE

Form Approved
OMB No. 0704-0188

1. AGENCY USE ONLY (Leave blank)	2. REPORT DATE	3. REPORT TYPE AND DATES COVERED
	May 1993	Technical Memorandum

4. TITLE AND SUBTITLE

On Nonlinear Tollmien-Schlichting/Vortex Interaction in Three-Dimensional Boundary Layers

5. FUNDING NUMBERS

WU–505–62–21

6. AUTHOR(S)

Dominic A.R. Davis and Frank T. Smith

7. PERFORMING ORGANIZATION NAME(S) AND ADDRESS(ES)

National Aeronautics and Space Administration
Lewis Research Center
Cleveland, Ohio 44135–3191

8. PERFORMING ORGANIZATION REPORT NUMBER

E–7889

9. SPONSORING/MONITORING AGENCY NAME(S) AND ADDRESS(ES)

National Aeronautics and Space Administration
Washington, D.C. 20546–0001

10. SPONSORING/MONITORING AGENCY REPORT NUMBER

NASA TM–106184
ICOMP–93–17

11. SUPPLEMENTARY NOTES

Dominic A.R. Davis, Institute for Computational Mechanics in Propulsion, Lewis Research Center (work funded under NASA Cooperative Agreement NCC3–233); Frank T. Smith, University College London, Gower Street, London, WC1E 6BT, United Kingdom. ICOMP Program Director, Louis A. Povinelli, (216) 433–5818.

12a. DISTRIBUTION/AVAILABILITY STATEMENT

Unclassified - Unlimited
Subject Category 34

12b. DISTRIBUTION CODE

13. ABSTRACT *(Maximum 200 words)*

The instability of an incompressible three-dimensional boundary layer (that is, one with cross-flow) is considered theoretically and computationally in the context of vortex/wave interactions. Specifically the work centres on two low-amplitude, lower-branch Tollmien-Schlichting waves which mutually interact to induce a weak longitudinal vortex flow; the vortex motion, in turn, gives rise to significant wave-modulation via wall-shear forcing. The characteristic Reynolds number is taken as a large parameter and, as a consequence, the waves' and the vortex motion are governed primarily by triple-deck theory. The nonlinear interaction is captured by a viscous partial-differential system for the vortex coupled with a pair of amplitude equations for each wave pressure. Three distinct possibilities were found to emerge for the nonlinear behavior of the flow solution downstream - an algebraic finite-distance singularity, far-downstream saturation or far-downstream wave-decay (leaving pure vortex flow) - depending on the input conditions, the wave angles and the size of the cross-flow.

14. SUBJECT TERMS

Vortex/wave interaction; Transition; Tollmien-Schlichting

15. NUMBER OF PAGES

29

16. PRICE CODE

A03

17. SECURITY CLASSIFICATION OF REPORT	18. SECURITY CLASSIFICATION OF THIS PAGE	19. SECURITY CLASSIFICATION OF ABSTRACT	20. LIMITATION OF ABSTRACT
Unclassified	Unclassified	Unclassified	